

# Lumped Element $Y$ Circulator

YOSHIHIRO KONISHI, SENIOR MEMBER, IEEE

**Abstract**—A lumped element  $Y$  circulator using ferrite, having a mesh mechanism in place of the center conductor of an ordinary  $Y$  strip line circulator, is proposed. A theory is developed relating to bandwidth, insertion loss, and temperature dependence of the reactive energy and the tensor permeability of ferrite, and the bandwidth enlargement is discussed on the basis of the equivalent network.

The size of the circulator is approximately 1~2 cm in diameter for VHF and UHF bands and the characteristics are, for example, about 50 percent bandwidth for 20-dB isolation, 2-dB insertion loss at 600-Mc/s center frequency. It is also shown that the insertion loss has its minimum value at a definite bandwidth and, as a practical example, a circulator is described with 0.25 dB of insertion loss and 6.5 percent bandwidth at 700 Mc/s.

## I. INTRODUCTION

The ordinary  $Y$  strip-line circulator [1]–[3] requires a ferrite with suitable diameter to keep its wide bandwidth and lossless characteristics, and recently, a miniaturized circulator available to the receiver has been required for the purpose of reducing the radiation of the local oscillator.

This paper presents the theory to synthesize the lumped element  $Y$  circulator having the proposed mechanism [4] and also the experimental results to confirm the theory.

This circulator is approximately 2~3 cm in diameter as shown on the photograph and the ferrite used is about 1~1.5 cm in diameter and 1~2 mm thick.

The center frequency of the circulator is adjustable by changing only the values of capacitances added at each terminal without changing the applied dc field and also internal mechanism around the ferrite. The experiment is made in the frequency range from about 10 Mc/s~1000 Mc/s.

The theories are given especially for the relationship between a bandwidth, forward loss, and reactive energy corresponding to the eigenvector excitations.

These quantities are also connected to the complex tensor permeability of the ferrite to make it possible for the characteristics of the circulator to be estimated by the material used in it. Furthermore, the equivalent network of this circulator is obtained and the wide-band circulator with Chebyshev and Wagner characteristics is synthesized in the same way as the band-pass filter design, together with its previously mentioned equivalent network. As a practical example, the circulator with about 50 percent in bandwidth for 20 dB isolation at a center frequency 600 Mc/s is designed,

and a small insertion loss circulator, one with 0.25 dB insertion loss at a center frequency 700 Mc/s is also shown.

The lumped element circulator has also been developed in the U.S.A. by V. Dunn and R. W. Robert.<sup>1</sup>

## II. CONSTRUCTION AND ITS EIGENVALUES

Figure 1 shows the construction of the inside of the circulator.

Three conductors connected to corresponding terminal of the circulator are insulated from each other and knitted together to form a mesh and are connected to earth at the other end. The mesh mechanism contributes to maintain circularly rotating  $rf$  field over the entire disk for the rotating field excitation, and since most of  $rf$  magnetic field passes through two ferrite disks as shown in Fig. 2, the leakage inductance, which prevents the circulator's bandwidth from becoming broad, can be avoided. The symmetrical structure about the mesh plane can keep the radiation loss small.

This rotationally symmetrical circuit has the eigenvector of (1) [5], and its eigenvalues  $Z_i'$  of  $Z$  matrix can be expressed in terms of the magnetic and electric energy for the unit current excitation corresponding to the  $i$ th eigenvector. (See Appendix I.)

$$\mathbf{u}_1 = \begin{bmatrix} 1 \\ 1 \\ 1 \end{bmatrix}, \quad \mathbf{u}_2 = \begin{bmatrix} 1 \\ \alpha^2 \\ \alpha \end{bmatrix}, \quad \mathbf{u}_3 = \begin{bmatrix} 1 \\ \alpha \\ \alpha^2 \end{bmatrix}. \quad (1)$$

However, when equal current flows only in conductors  $1a$  and  $1b$  in Fig. 2, the  $rf$  magnetic field surrounds  $1a$  and  $1b$  through the mesh between  $2a$ ,  $2b$ ,  $3a$ , and  $3b$  as in Fig. 2(b), and is distributed almost uniformly on the ferrite surface as shown in Fig. 2(a). Simplifying the analysis, we take the simple assumption that the distribution of the field is completely parallel with the direction perpendicular to  $1a$  and  $1b$ , although there exist the other higher modes to satisfy the boundary condition. We also assume the diameter is sufficiently small to be able to neglect the variation of the field intensity along  $1a$  and  $1b$ , so that we can neglect the electric energy inside the ferrite compared with the magnetic energy. Under the assumption mentioned before,  $Z_i'$  in the part of ferrite without  $C$  added at each terminal can be expressed by (2) from the result in Appendix I.

Manuscript received February 11, 1965; revised August 9, 1965.  
The author is with Technical Research Labs., Japan Broadcasting Co., Tokyo, Japan.

<sup>1</sup> See their article, "Miniature VHF-UHF circulators use lumped-element design," *Microwave J.*, pp. 46–47, December 1963.

$$Z_i' = j \frac{\omega}{3} \iiint_{\tau} H_i^* \mathbf{u} H_i d\tau \quad (2)$$

where

$\tau$ : the integrated region of ferrite

$$\mathbf{u} = \begin{bmatrix} \mu & -jk & 0 \\ jk & \mu & 0 \\ 0 & 0 & 1 \end{bmatrix} : \text{tensor permeability of ferrite with the dc magnetic field in the } Z \text{ direction}$$

$E_i, H_i$ : high frequency electric and magnetic fields in the ferrite when it is excited by constant current of  $i$ th eigenvector

$\omega$ : angular frequency.

The frequency variation of  $Z_i', \delta Z_i'$  is (see Appendix II)

$$\delta Z_i' = j \frac{\delta\omega}{3} \iiint_{\tau} H_i^* \left( \mathbf{u} + \frac{\partial \mathbf{u}}{\partial \omega} \omega \right) H_i d\tau. \quad (3)$$

In VHF and UHF circulators, the applied dc magnetic field should be much stronger than the resonance field in order to make it of low forward loss. In this case, we can apply the relation  $(\partial \mathbf{u} / \partial \omega) \omega \ll \mathbf{u}$  in (3). Taking account of the assumption of the field uniformity, the 2nd and 3rd eigenvector currents give the complete negative and positive rotating field inside ferrite. So, we get

$$Z_i' = j\omega L_i, \quad L_i = \mu_i \xi,$$

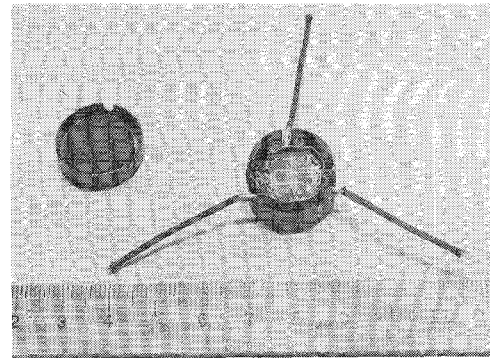
$$\xi = \frac{1}{3} \iiint_{\tau} |H_i|^2 d\tau, \quad (\mu_2 = \mu_-, \mu_3 = \mu_+)$$

from (2) and (3) where  $\xi$  is independent of frequency.

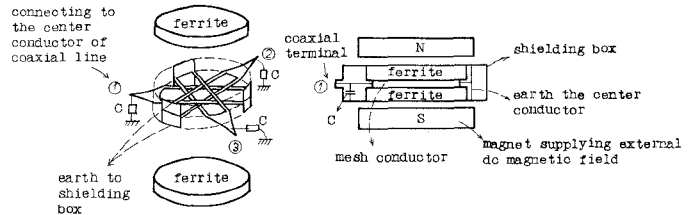
The 1st eigenvector currents give rise to no magnetic field inside the ferrite. This results in  $Z_1 = 0$ , which has been confirmed by experiments, as in Fig. 4, to be satisfactory in the VHF-UHF region. To examine the value of  $\mu_i$ , the values of  $Z_2'$  and  $Z_3'$  are measured for dc magnetic field of several strengths, and the measured values  $Z_2' / j\omega \xi = \mu_-$  and  $Z_3' / j\omega \xi = \mu_+$  are plotted with a sign of  $\times$  in Fig. 3, where  $j\omega \xi$  are the values of  $Z_2', Z_3'$  under the dc magnetic field strong enough to saturate the  $\mu_{\pm}$  values to one. The measuring technique is shown in Appendix III. The line in Fig. 3 shows the calculated values of  $\mu_+$  and  $\mu_-$  by Polder's equation (15), and it shows good coincidence with measured values. This makes it possible not only to substitute  $\mathbf{u}$  by  $\mu_+$  and  $\mu_-$ , at least in the discussion of their relative values, but also to use (15) for analysis in introducing the design formula.

Therefore, considering the capacities at each terminal, the eigenvalues are expressed in the equivalent admittances in

$$y_1 = \infty, y_2 = j\omega c + \frac{1}{j\omega \mu_- \xi}, y_3 = j\omega c + \frac{1}{j\omega \mu_+ \xi}. \quad (4)$$

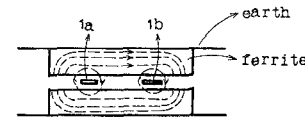


(a)

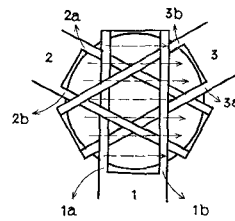


(b)

Fig. 1. (a). Photograph of lumped element Y circulator (scale indicates dimensions in cm). (b) Construction of proposed lumped element Y circulator. Left side—construction inside shielding box. Right side—sectional view in the plane including terminal ① and center axis.



(a)



(b)

Fig. 2. Field distribution inside ferrite by currents on 1(a) and (b).

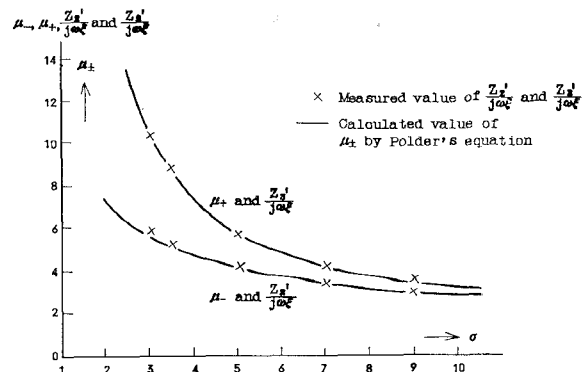


Fig. 3. Measured values of  $Z_2' / j\omega \xi$  and  $Z_3' / j\omega \xi$  at 150 Mc/s plotted by  $\times$  signs, and calculated values of positive and negative polarized permeabilities  $\mu_{\pm}$  shown by lines.

When

$$y_2 = -j \frac{1}{\sqrt{3}}, \quad y_3 = j \frac{1}{\sqrt{3}},$$

a circulator is realized, where the terminal impedance is normalized to one ohm as simplification, and the normalization is also made throughout Section III.

The measured eigenvalues are shown on the Smith chart with an arrowed line in Fig. 4.

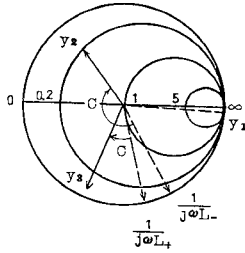


Fig. 4. Measured values of eigenvalues.  
 $\leftarrow$  — — — before connecting  $C$ .  
 $\leftarrow$  — after connecting  $C$ .

### III. ELECTRICAL CHARACTERISTICS

#### A. Bandwidth and Insertion Loss

The variation of eigenvalues  $\delta s_i$  takes place by the variation of frequency  $\delta\omega$  from the center frequency, and the signal is transmitted also backward in the amount of  $|S''|$  for the unit amplitude of the incident signal. The relation between  $|S''|$  and  $|\delta s_i|$  can be obtained as shown in

$$|S''| = \frac{1}{3} \sqrt{\sum_{i=1}^3 |\delta s_i|^2 - \sum_{\substack{i,j=1 \\ i \neq j}}^3 |\delta s_i| \cdot |\delta s_j|}. \quad (5)$$

Nevertheless, there are relations of (6), between  $s_i$ ,  $y_i$  and their frequency variations  $\delta s_i$ ,  $\delta y_i$ ;

$$s_i = \frac{1 - y_i}{1 + y_i}, \quad \delta s_i = \frac{-\delta y_i}{(1 + y_i)^2}. \quad (6)$$

It is easily understood in Fig. 4 that (7) must be satisfied to realize a circulator.

$$\omega c = \frac{1}{2} \left( \frac{1}{\omega \xi \mu_-} + \frac{1}{\omega \xi \mu_+} \right), \quad \frac{1}{\omega \xi \mu_-} - \frac{1}{\omega \xi \mu_+} = \frac{2}{\sqrt{3}}. \quad (7)$$

Substituting (4) and (6) into (5), and applying the relation of (7) to it,  $|S''|$  can be expressed in terms of  $C$  and  $\mu_{\pm}$ . It can be also connected to the time average total reactive energy  $\bar{W}_t$  stored inside the circulator in the case of constant voltage eigenvector  $\mathbf{u}_2$  and  $\mathbf{u}_3$  with unit amplitude.

The previously mentioned results, are shown in (8). (See Appendix IV.)

$$\begin{aligned} w &= \frac{2|S''|}{\omega C \sqrt{1 + \frac{1}{(2\omega C)^2}}} = \frac{2\sqrt{3}|S''|\eta}{\sqrt{1 + \frac{3}{4}\eta^2}} \\ &= \frac{6|S''|}{\omega \bar{W}_t \sqrt{1 + \left(\frac{3}{2\omega \bar{W}_t}\right)^2}} \\ \eta &= \frac{\mu_+ - \mu_-}{\mu_+ + \mu_-}. \end{aligned} \quad (8)$$

In (8)  $w$  is the bandwidth normalized to the center frequency, at which the backward transmission is kept in the amount of desired values  $|S''|$ . Equation (8) shows that the bandwidth becomes narrower for the circulator with large  $C$ , when the required dc magnetic field should be stronger and ferrite operate at small  $\eta$ . In this operation, the corresponding reactive energy becomes larger.

Next, considering the quality factor of the permeability of the ferrite and the permittivity of  $C$ , the added capacitors at each terminal, we put

$$\mu_{\pm} = \mu_{\pm}' \left( 1 - j \frac{1}{Q_{\pm}} \right), \quad C = C' \left( 1 - j \frac{1}{Q_c} \right). \quad (9)$$

Substituting (9) into (4), we get the amount of forward loss as in (10)

$$\begin{aligned} L(\text{dB}) &= \frac{4.96}{\eta Q_c} + \frac{2.48}{Q_+} \left( \frac{1}{\eta} - 1 \right) \\ &\quad + \frac{2.48}{Q_-} \left( \frac{1}{\eta} + 1 \right). \end{aligned} \quad (10)$$

However, we have the relation between  $\mu_{\pm}$  and  $\mu_{\text{eff}}$  and the loss term of  $\mu_{\text{eff}}$  is expressed by its quality factor  $Q_{\text{eff}}$  as in

$$\mu_{\text{eff}} = \mu_{\text{eff}}' \left( 1 - \frac{1}{Q_{\text{eff}}} \right) = \frac{\mu^2 - \kappa^2}{\mu} = \frac{2}{\frac{1}{\mu_+} + \frac{1}{\mu_-}}. \quad (11)$$

Substituting (9) into (11) one gets

$$\frac{1}{Q_{\text{eff}}} = \frac{\eta}{2} \left[ \left( \frac{1}{\eta} - 1 \right) \frac{1}{Q_+} + \left( \frac{1}{\eta} + 1 \right) \frac{1}{Q_-} \right]. \quad (12)$$

From (10) and (12), the insertion loss  $L$  (dB) can be expressed by the simpler form with  $Q_{\text{eff}}$  as in

$$L(\text{dB}) = \frac{4.96}{\eta} \left( \frac{1}{Q_c} + \frac{1}{Q_{\text{eff}}} \right). \quad (13)$$

In (13), when dc magnetic field becomes stronger,  $Q_{\text{eff}}$  becomes larger and  $\eta$  smaller. So,  $L$  (dB) takes its minimum value at the proper strength of dc magnetic field, and this is determined by applying the measured values of  $Q_{\text{eff}}$  and  $\eta$  into (13) together with the value of  $Q_c$ ,

where  $\eta$  is obtainable from the measured values of  $\mu_{\text{eff}}$  by the relation of

$$\eta = \frac{P}{\sigma(P + \sigma) - 1}, \quad \mu_{\text{eff}} = \frac{(\sigma + P)^2 - 1}{\sigma(\sigma + P) - 1}. \quad (14)$$

The methods of the measurement of  $Q_{\text{eff}}$  and  $\mu_{\text{eff}}$ , and the determination techniques are described in Appendix V. A practical example is shown in Section VII.

### B. Adjustment of Center Frequency by Changing $C$

When the formula of (15) for  $\mu_i$  is used,

$$\mu_i = 1 + \frac{P}{\sigma + (-1)^i}, \quad (\mu_2 = \mu_-, \mu_3 = \mu_+)$$

$$\sigma = \frac{|\gamma| H_0}{\omega}, \quad P = \frac{4\pi M_s |\gamma|}{\omega}, \quad (15)$$

where  $\gamma$  is gyro magnetic ratio and  $4\pi M_s$  is saturation magnetization. The difference between both admittances of  $L_+$  and  $L_-$  becomes independent of  $\omega$  for  $\sigma^2 \gg 1$ , or  $P^2 \gg 1$ , where the former is satisfied in the case of strong dc field and the latter in the case of the low frequency as VHF band (Appendix VI).

Therefore, the circulator is always realized only by adjusting  $C$  proportional to  $\omega^2$  as in (16)

$$C = \frac{|\gamma| H_0}{\sqrt{3} \omega^2} \left( 1 + \frac{H_0}{4\pi M_s} \right). \quad (16)$$

Substituting (16) into (10), the bandwidth  $w$  of this circulator is obtained in (17). It is understood that  $w$  becomes wide proportional to the center frequency and inversely proportional to  $\sigma$ .

$$w = \frac{2\sqrt{3} |S''| \omega}{\left( 1 + \frac{H_0}{4\pi M_s} \right) |\gamma| H_0} = \frac{2\sqrt{3} |S''|}{\sigma \left( 1 + \frac{\sigma}{P} \right)}. \quad (17)$$

Substituting (15) into (9), the value of  $\xi$  is obtained in

$$\omega \xi = \frac{\sqrt{3}}{2} \left( \frac{1}{\mu_-} - \frac{1}{\mu_+} \right) = \frac{\sqrt{3} P}{(\sigma + P)^2 - 1},$$

$$\sigma = \frac{|\gamma| H_0}{\omega}. \quad (18)$$

Therefore, the result of the measurement, in advance of  $\xi$  for several sizes of the mesh part, is available to decide the size of the mesh part and also ferrite disks required from (18). The measured values of  $\xi$  are indicated in Fig. 5, where  $t$  is the thickness of the ferrite disk.

While the previous description has been concerned with constant applied dc magnetic field, the situation with stronger dc magnetic field will be considered. In this case the larger value of  $C$  and the smaller value of  $\xi$  are required even at the same frequency and the bandwidth of  $w$  becomes smaller.

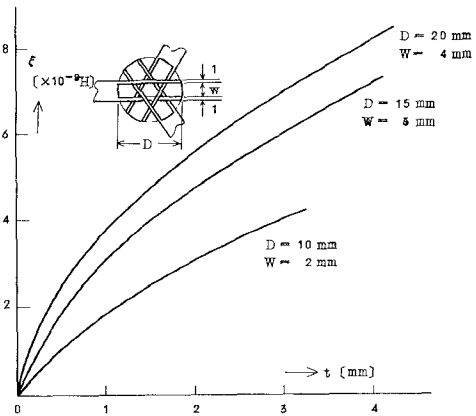


Fig. 5. Measured values of  $\xi$  of mesh part with several sizes, where  $\xi$  is the value  $Z_1/j\omega$  when the strong dc magnetic field is applied to saturate  $\mu_{\pm}$  to one.  $t$  is width of the part for the insertion of ferrite disks.

## IV. THE SYNTHESIS OF WIDE-BAND LUMPED ELEMENT $Y$ CIRCULATOR

### A. Equivalent Circuit of Lumped Element $Y$ Circulator

Taking the variation of  $y_i$  in (6) and applying (15) and its variation  $\delta\mu_i$ , we get the relation of

$$\delta y_i = j\delta\omega \left[ C + \frac{1}{\omega^2 \mu_i \xi} \cdot \left\{ 1 - \frac{(-1)^i P}{(\sigma + (-1)^i)(\sigma + P + (-1)^i)} \right\} \right].$$

For  $P$  and  $\sigma \gg 1$ ,  $\delta y_2$  and  $\delta y_3$  take the same value of (19).

$$\delta y_2 = \delta y_3 = j \left\{ \omega C + \frac{1}{\omega \xi \left( 1 - \frac{P}{\sigma} \right)} \right\} \frac{\delta\omega}{\omega}. \quad (19)$$

However,  $y_1$  takes always infinite value at any frequency. Under these conditions, that is,

$$\delta y_2 = \delta y_3, \quad y_1 = \infty, \quad \delta s_1 = 0, \quad (20)$$

the equivalent network has the construction consisting of one ideal circulator available to any frequency and three parallel tuned circuits connected at each terminal of the ideal circulator which is illustrated in the part surrounded by the dotted line in Fig. 6.

The frequency variation of the 2nd and the 3rd eigenvalues of  $Y$  matrix coincides with frequency variation of the parallel tuned circuits connected at each terminal, and  $\delta y_2 = \delta y_3$  because they are reciprocal circuits. On the other hand, the 1st eigenvalues are not affected by the tuned circuits because they are connected at the zero impedance point of the 1st eigenvalue. So it satisfies the condition of  $y_1 = \infty$ ,  $\delta s_1 = 0$ . From this reason, this equivalent network satisfies all the conditions described in (20).

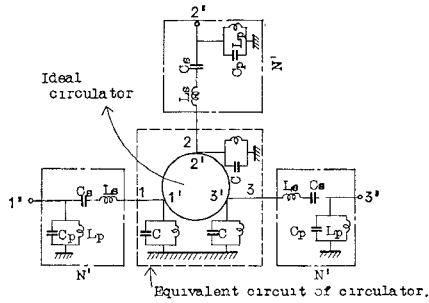


Fig. 6. Equivalent network of circulator and added network for wideband.  $N'$  is the network for wideband operation where  $cp$ ,  $Lp$  are not necessary for  $N=2$ .

### B. Bandwidth Enlargement with Chebyshev Characteristics

Let the terminals of the ideal circulator be  $1'$ ,  $2'$ , and  $3'$  as shown in Fig. 6. We consider the purely reactive four-terminal networks  $N'$  connected to each terminal 1, 2, 3 of the circulator and name the outside terminals of  $N'$ ,  $1''$ ,  $2''$ ,  $3''$  respectively. Let the network, which contains  $N'$  and the parallel tuned circuits at terminals 1, 2, 3 be named  $N$ . When the terminals  $2''$  and  $3''$  are terminated with matched loads and an incident signal with unit amplitude is applied to terminal  $1''$ , it comes out of terminal  $3'$ . If there is a reflection in the amount of  $\Gamma$  at terminal  $3'$ , the reflected wave caused by  $\Gamma$  is transmitted again toward terminal 2 through the ideal circulator. Hence  $|S''| = \Gamma$ . Between  $|\Gamma|$  and power-loss ratio of  $N$ ,  $P_0/P_L$ , we have the relation of

$$\frac{P_0}{P_L} = \frac{1}{1 - |\Gamma|^2} = 1 + \frac{1}{\frac{1}{|\Gamma|^2} - 1}$$

Therefore, to keep  $|S''|$  below the value  $|S''_{\max}|$  throughout the frequency band between  $\omega_1'$  and  $\omega_2'$ , the network  $N$  should be designed with its power-loss ratio satisfying the requirements of a band-pass network with proper characteristics. In this section, the Chebyshev characteristics of (21) are discussed.

$$\left. \begin{aligned} \frac{P_0}{P_L} &= 1 + h^2 T_n^2(\omega') \\ \omega' &= \frac{\omega_c}{K} \left( \frac{\omega}{\omega_0} - \frac{\omega_0}{\omega} \right) \\ \omega_1 &= \frac{1}{2} \left\{ -K\omega_c + \sqrt{(K\omega_c)^2 + 4\omega_0^2} \right\} \\ \omega_2 &= \frac{1}{2} \left\{ K\omega_c + \sqrt{(K\omega_c)^2 + 4\omega_0^2} \right\} \end{aligned} \right\} \quad (21)$$

where  $h$  is a constant determining the maximum insertion loss in a pass band,  $K$  is a constant relating the bandwidth of a band-pass filter to that of a low-pass filter, and  $T_n$  is a first kind  $n$ th order Chebyshev polynomial. In (21)  $h$  is related to minimum backward loss  $A$  dB by

$$h = \frac{1}{\sqrt{10^{A/10} - 1}}, \quad A = 20 \log_{10} \frac{1}{|S''_{\max}|} \quad (22)$$

These characteristics are synthesized from ordinary low-pass filter theory [7] and realized by ladder networks in which the series and parallel elements are, respectively, the series- and parallel-resonance circuits tuned to center frequency  $\omega_0$ , where  $\omega_0$  is obtained from  $\omega_0^2 = \omega_1' \omega_2'$ . When the total number  $n$  of all resonance circuits is odd, the input and output impedances of  $N$  take the same value, while they take different values when  $n$  is even. The network must always be synthesized in such a way that the 1st element is a parallel element, because the parallel tuned circuit of the equivalent network of a circulator is always put as the first element of network  $N$ .

The bandwidth is increased more with the increasing of  $n$ , and the results of the calculations are shown in Table I for the cases of backward loss  $A$  equal to 20 dB and 30 dB. It is seen that the improvement in bandwidth is much less remarkable for  $n$  larger than 2 or 3. Moreover, they are the most useful numbers of elements in practical components for VHF and UHF bands. So, only the results of  $n=2$  and  $n=3$  are shown in this paper. (For  $n > 3$ , refer to (8).)

TABLE I  
RELATION BETWEEN  $n$  AND BANDWIDTH INCREASING RATIO  $w_n/w_1$

$n$	$A=20$ dB	$A=30$ dB
1	1	1
2	3.55	5.7
3	4.25	8.42
4	4.47	9.63
5	4.633	10.6
$\infty$	6.16	14.3

$A$  is the minimum backward loss in the specified bandwidth.

#### 1) In the case of $n=2$

The network for the wide bandwidth consists of only the series-resonance circuit connected in series at each terminal, of which inductance  $L_s$  and capacitance  $C_s$  take the values shown in (23).

$$\begin{aligned} L_s &= 1 + \frac{4}{\xi^2} R^2 C, & C_s &= \frac{1}{\omega_0^2 L_s} \\ \xi &= \left( \frac{2}{a} \right)^{1/4} - \left( \frac{2}{a} \right)^{-1/4}, \\ a &= \frac{1}{2(10^{A/10} - 1)} = \frac{h^2}{2} \end{aligned} \quad (23)$$

where  $R$  is the terminal impedance of the wide-band circulator.

In this circulator, the terminal impedance, before increasing the bandwidth by  $L_s$  and  $C_s$ , must be  $R_e$ , which takes a slightly different value from  $R$  as shown in

$$R_e = \frac{1 + \sqrt{2a}}{1 - \sqrt{2a}} R \quad (24)$$

This has the physical meaning that the circulator does not have infinite backward loss at a center frequency but at frequencies deviating slightly from the center.

The bandwidth is increased in the amount of 3.55 times for  $A=20$  dB and 5.7 times for  $A=30$  dB as shown in Table I. This is in good agreement with the experiment which will be described later.

2) In the case of  $n=3$

The network constitutes one series-resonance circuit connected first in series, and one parallel-resonance circuit connected next in parallel as indicated in Fig. 6. The values in (25) denote the inductance and capacitance of series resonance,  $L_s$  and  $C_s$ , and those of parallel resonance,  $L_p$  and  $C_p$ ,

$$\begin{aligned} L_s &= \frac{2\zeta^2}{\zeta^2 + 3/4} R^2 C, & C_s &= \frac{1}{\omega_0^2 L_s} \\ L_p &= \frac{1}{\omega_0^2 C}, & C_p &= C \end{aligned} \quad (25)$$

where  $\zeta$  takes the same value as in (23). In this circulator, the terminal impedance, before increasing the bandwidth, is equal to that of the increased bandwidth. This means that the backward loss must be adjusted to infinite value at the center frequency. The bandwidth is theoretically increased 4.25 times for  $A=20$  dB and 8.42 times for  $A=30$  dB as indicated in Table I.

C. Bandwidth Enlargement with Wagner Characteristics

The power-loss ratio of network  $N$  takes the form of

$$\frac{P_0}{P_L} = 1 + \omega'^{2n} \quad (26)$$

$\omega'$  is the same one used in (21) and shows the angular frequency corresponding to that translated into the low-pass filter. The network construction is similar to the Chebyshev type with only the exception of their constants. The terminal impedance before enlarging the bandwidth is the same as that for the enlarged bandwidth. The circuit constants and the bandwidth increasing ratio for  $n=2, 3$  are shown in (27).

- 1)  $n=2$ , series elements  $L_s = CR^2, C_s = \frac{1}{\omega_0^2 L_s}$   
the bandwidth increasing ratio =  $\sqrt{5}$
- 2)  $n=3$ , series elements  $L_s = 2CR^2, C_s = \frac{1}{\omega_0^2 L_s}$   
parallel elements  $L_p = \frac{1}{\omega_0^2 C_p}, C_p = C$   
the bandwidth increasing ratio = 2.33. (27)

V. TEMPERATURE DEPENDENCE

The temperature dependence of a circulator is caused mainly by the deviation of the external dc magnetic field  $H_{ex}$  and the saturation magnetization  $M_s$  of the ferrite following the fluctuation of temperature.

The dc magnetic field  $H_0$  inside the ferrite is also decreased from  $H_{ex}$  by the demagnetizing field in the amount of (28) for the ellipsoidal ferrite.

$$H_0 = H_{ex} - N_z \cdot M_s, \quad (28)$$

$N_z$  is the demagnetizing factor in the  $Z$  direction. Equation (28) shows  $H_0$  is affected by the change of  $H_{ex}$  and also  $M_s$ . Then  $\mu_{\pm}$  vary their values by the change of  $M_s$  and  $H_0$  following (15). These variations of permeability result in the deviation of the 2nd and the 3rd eigenvalues. Therefore, the center frequency of the circulator deviates, causing the backward loss at the operating center frequency to be changed by a variation of temperature. These temperature dependencies are quantitatively described in the following section.

A. Deviation of Center Frequency

The variation of  $\mu, \delta\mu$ , is obtained from (15) as

$$\left. \begin{aligned} \delta\mu_{-} &= \frac{\pm P}{(\sigma \mp 1)^2} \cdot \frac{\delta\omega}{\omega} + \frac{P}{\sigma \mp 1} \left( 1 + \frac{PN_z}{\sigma \mp 1} \right) \frac{\delta(4\pi M_s)}{4\pi M_s} \\ P &= \frac{4\pi M_s |\gamma|}{\omega}, & \sigma &= \frac{|\gamma| (H_{ex} - N_z M_s)}{\omega} \end{aligned} \right\} \quad (29)$$

$\delta(4\pi M_s)$  shows the deviation of  $4\pi M_s$  caused by the change of temperature. As  $y_2$  and  $y_3$  are functions of  $\mu_{\pm}$  and  $\omega$ , their variation becomes

$$\delta y_i = j \frac{\delta\omega}{\omega} \left( \omega C + \frac{1}{\omega \xi \mu_i} \right) + \frac{j}{\omega \xi \mu_i} \cdot \frac{\delta\mu_i}{\mu_i}, \quad (\mu_2 = \mu_{-}, \mu_3 = \mu_{+}). \quad (30)$$

However, as  $\delta s_1=0$  as mentioned before, we have to apply the conditions  $\delta s_2=\delta s_3=0$  and  $\delta y_2=\delta y_3=0$  for satisfying the condition of the circulator. Substituting this relation into (30) and (29), one can get the deviation of the center frequency  $\delta\omega$ . Taking the approximations of  $N_z=4\pi$  for thin ferrite disks,  $\sigma \gg 1$  and  $\omega C \doteq 1/\omega \xi_{\mp} \mu$ , we get

$$\frac{\delta\omega}{\omega} = \frac{\delta(4\pi M_s) - \frac{P}{\sigma + P} \delta H_{ex}}{2H_0}. \quad (31)$$

From (31), it is understandable that  $\delta\omega$  is smaller for the circulator operating under the stronger  $H_{ex}$ . This means the effect of the demagnetizing field is small in this case.

B. Change of Backward Loss at Center Frequency Depending upon Temperature

As  $s_1$  is independent of permeability, the variation for temperature  $\delta s_1$  is also zero. Substituting  $\delta s_1=0$  into (5) and considering the conditions  $y_1 = \infty, y_2 = -j/\sqrt{3}, y_3 = j/\sqrt{3}$ , and the relation of (6), one gets

$$|S'''| = \frac{1}{2} \sqrt{|\delta y_2|^2 - |\delta y_3|^2 - |\delta y_2| \cdot |\delta y_3|}. \quad (32)$$

As we consider the state at the same frequency,  $\delta y_i$  in (32) means the variation of  $y_i$  for only the variation of temperature and coincides with one substituted by  $\delta\omega=0$  into the 1st term of (30). Also  $\delta\mu_i$  is obtained by putting  $\delta\omega=0$  into (29). That is,

$$\delta y_i = \frac{j}{\omega\xi\mu_i} \cdot \frac{\delta\mu_i}{\mu_i} \quad (33)$$

$$\delta\mu_i = \frac{P(P+\sigma)}{\sigma^2} \cdot \frac{\delta(4\pi M_s)}{4\pi M_s} \quad (34)$$

Substituting (34) and the value of  $\omega\xi$  of (18) into (33), and putting these results into (32), one gets the value of  $|S''|$  in

$$|S''| = \frac{1}{2\sqrt{3}} \left( 1 + \frac{\sigma}{P} \right) \frac{\delta(4\pi M_s)}{H_{res}} \quad (35)$$

It shows the circulator for the smaller frequency is more sensitive for the variation of temperature because  $H_{res}$  is proportional to  $\omega$  in (35).

## VI. DESIGN PROCEDURE AND ITS PRACTICAL EXAMPLE

On the basis of the previous results, the design can be approached in the several ways. As an example, one can start with a specified bandwidth, or one can also design with a minimum insertion loss by operating under the optimum  $\sigma$  as described in 3A. The process for the former case is shown in Table II, where design formulas available to terminal impedance of  $R_e$ , are shown, though it has been normalized to one ohm in Section II and III.

As a practical problem, there exist some capacitances between conductors in the mesh part, and they work as a part of  $C$  at each terminal by 3 times its value. Therefore, it must be subtracted from the value of  $C$  calculated by Table II in advance for practical design, which takes different values depending mainly on the gap between conductors, actually being about 3–6 pF as determined by experiment.

### Practical Example

We design a circulator which has a backward loss of 20 dB in the frequency range from 170 Mc/s to 230 Mc/s. A YIG polycrystalline material is used which has a  $4\pi M_s$  of 1,000 Gs. The bandwidth ratio  $w=0.3$  (30 percent). Following Table II,

- 1)  $w_1=0.3/3.55=0.0845$  for  $n=2$ ,
- 2)  $\eta=0.25$ ,
- 3)  $C=31.4$  pF
- 4)  $L_S=0.113$   $\mu H$ ,  $C_S=5.6$  pF,  $R_e=60\Omega$ ,
- 5)  $P=10$  (measured value of  $|\gamma|/2\pi=2$  Mc/Oer is used), so  $\sigma=3.13$

- 6)  $\xi=3.9$   $m\mu H$

- 7)  $D=1.5$  mm  $t=1.5$  mm from Fig. 5,  $t$  is thickness of ferrite disk.

Required capacitance at each terminal  $C$  is 25 pF, considering the floating capacitance mentioned before. The results of experiment, shown in Fig. 7(a), show good agreement with the specified characteristics.

## VII. RESULT OF EXPERIMENT

### A. Experimental Results of VHF and UHF Wide-Band Circulator

Figure 7(a) is an example designed from results obtained in Section VI. The same experimental result in UHF band is illustrated in Fig. 7(b).

### B. Variation of Center Frequency by Changing the Value of $C$

The experimental results of the adjustment of the center frequency by changing only the value of  $C$ , are shown in Fig. 8. It is understandable that the relationship between the values of  $C$  and the frequency, and also between  $w$  and the frequency are well satisfied by (16) and (17). The experiment was also performed on the circulator with the insertion loss of 2 dB and 1 per cent bandwidth at a center frequency of 12 Mc/s.

### C. Determination of Inertion Loss and Bandwidth by Measurement of $Q_{eff}$ and $\mu_{eff}$ of Ferrite

$Q_{eff}$  and  $\mu_{eff}$  are measured at 700 Mc/s under several strengths of dc magnetic field, and the estimated values of  $L$ (dB) and  $w$  are indicated in Fig. 9(a). This shows that the minimum insertion loss is 0.15 dB and the corresponding bandwidth is 6.5 percent. The experimental result shows 0.25 dB of insertion loss and 6.5 percent bandwidth as shown in Fig. 8(b).

The same measurements were made at several frequencies; the minimum insertion loss and corresponding bandwidth  $w$  are indicated in Fig. 9(b). This figure shows that the insertion loss becomes larger with the decreasing of the frequency.

### D. Experiment on Temperature Dependence

Experiments were made on the temperature dependence of the circulator using MnMgAl ferrite disks and Ba-ferrite for  $H_{ex}$ . Its center frequency is 200 Mc/s, and the bandwidth is 17 Mc/s. The  $4\pi M_s$  of ferrite is 1200 Gs and its variation  $\delta(4\pi M_s)$  is 81 Gs for the temperature variation from 20°C to 50°C. Following the design formula of Table II for  $\sigma=3.35$ ,  $P=16.7$  and  $H_{res}=72.5$  Oer, we get  $H_{ex}=N_z \cdot M_s + H_{res}=1435$  Oer. Ba-ferrite biasing magnet has a temperature coefficient such a 0.052 decrease in  $H_{ex}$  from 20°C to 50°C. Putting these values into (31), we get  $\delta\omega/\omega=-4.1$  percent. The experimental results are shown in Fig. 10(a) and (b), making good coincidence with theoretical values.

TABLE II  
DESIGN PROCEDURE AND FORMULAS

	Evaluated Values and Formulas Used	Known Values	
1)	$w_1 = w_n / \text{Bandwidth Increasing Ratio}$ , the ratio is shown in Table I.	$w_n$ (specified bandwidth)	
2)	$\eta = \frac{w_1}{2\sqrt{3} S''  \sqrt{1 - \left(\frac{1}{4 S'' }\right)^2}} \doteq \frac{w_1}{2\sqrt{3} S'' }$	$w_1,  S'' $	Induced from (8)
3)	$C = \frac{2 S'' }{R_0\omega w_1} \sqrt{1 - \left(\frac{w_1}{4 S'' }\right)^2} \doteq \frac{2 S'' }{\omega w_1 R_e}$	$\omega, w_1,  S'' $	(8) is changed to that available to terminal impedance $R_e$ .
4)	<p>Network Constants for Wide Band. Cheb. Char.</p> <p><math>n = 2: L_s = \left(1 + \frac{4}{\zeta^2}\right) R^2 C, C_s = \frac{1}{\omega_0^2 L_s}, R_e = \frac{1 + \sqrt{2a}}{1 - \sqrt{2a}} R</math></p> <p><math>n = 3: L_s = \frac{2\zeta^2 R^2 C}{\zeta^2 + \frac{3}{4}}, C_s = \frac{1}{\omega_0^2 L_s}, L_p = \frac{1}{\omega_0^2 C_p}</math></p> <p><math>C_p = C, R_e = R</math></p> <p><math>\zeta = \left(\frac{2}{a}\right)^{1/4} - \left(\frac{2}{a}\right)^{-1/4}</math></p> <p><math>a = \frac{1}{2(10^{4/10} - 1)}</math></p> <p>Wag. Char.</p> <p><math>n = 2: L_s = CR^2, C_s = \frac{1}{\omega_0^2 L_s}</math></p> <p><math>n = 3: L_s = 2CR^2, C_s = \frac{1}{\omega_0^2 L_s}</math></p> <p><math>L_p = \frac{1}{\omega_0^2 C_p}, C_p = C</math></p>	<p><math>A</math> (Backward Loss)</p> <p><math>n</math>: order of Cheb. or Wag. char.</p>	$L_s, C_s, L_p, C_p$ are the element constants in Fig. 7
5)	$\sigma = \frac{P}{2} \left( \sqrt{1 + \frac{4(P + \eta)}{P^2 \eta}} - 1 \right) \doteq \frac{P}{2} \left( \sqrt{1 + \frac{4}{P\eta}} - 1 \right)$	$P = \frac{4\pi M_s  \gamma }{\omega}$ $\eta = \frac{\mu_+ - \mu_-}{\mu_+ + \mu_-}$	Induced from (15) and the definition of $\eta$ .
6)	$\xi = \frac{\sqrt{3} P R_e}{\omega \{(\sigma + P)^2 - 1\}} \doteq \frac{\sqrt{3} R_e}{\omega P \left(1 + \frac{\sigma}{P}\right)^2}$	$P, \sigma$	(18) is changed to that available to terminal impedance $R_e$ .
7)	Diameter $D(mm)$ and Thickness $l(mm)$ of ferrite are determined by the value of $\xi$ and Fig. 5.	$\xi$	
8)	$H_{ex} = \frac{\omega}{ \gamma } \sigma + N_z \cdot M_s$	$\omega, 4\pi M_s, N_z,  \gamma , \sigma$	

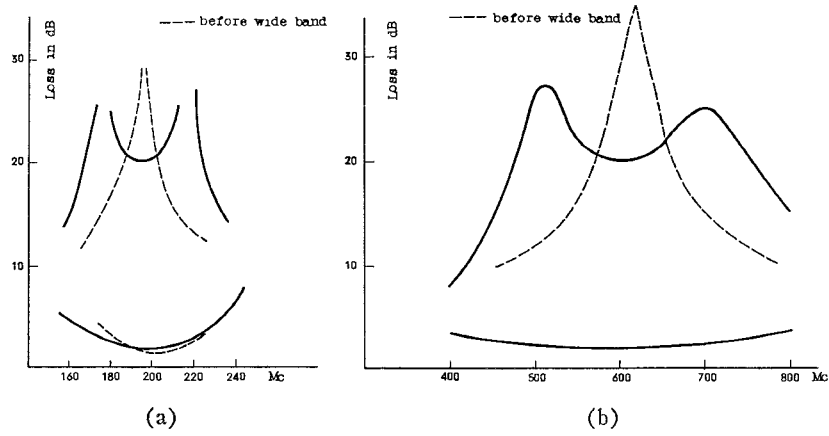


Fig. 7. Measured values of characteristics of wideband circulator with 2nd Chebyshev characteristic. (a) Experiment of VHF circulator. (b) Experiment of UHF circulator.

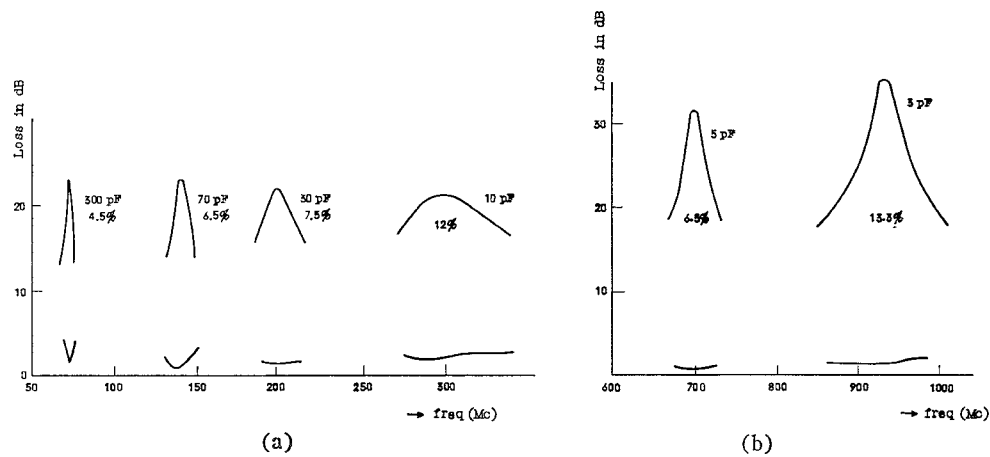


Fig. 8. Experimental results of VHF, UHF lumped element Y circulator. (a) Adjustment of center frequency by only changing C. (b) Experiment of UHF circulator.

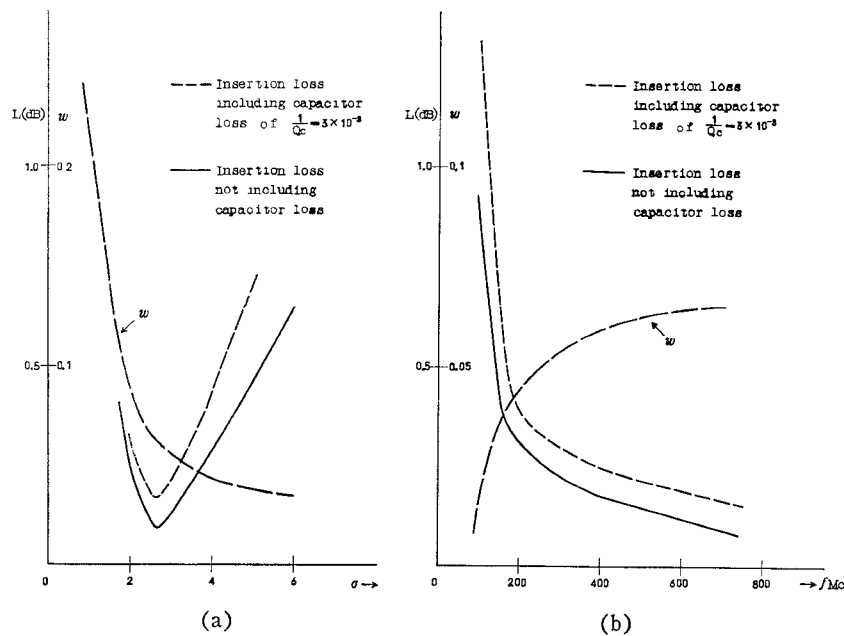


Fig. 9. Determination of characteristics of circulator by measurements of permeability and its quality factor of ferrite. (a) Determination of insertion loss and bandwidth of circulator at 700 Mc/s for several operations of dc magnetic field. (b) Determination of minimum insertion loss and bandwidth for several frequencies.

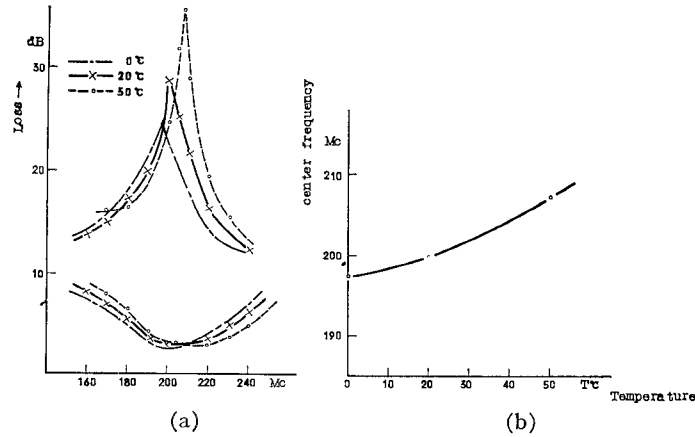


Fig. 10. Measurement of temperature dependence of circulator. (a) Deviation of backward and forward loss with temperature variation. (b) Deviation of center frequency with temperature variation.

### VIII. CONCLUSION

The miniaturized circulator available to VHF and UHF bands has been developed and we get good agreement between the theories and the experimental results.

The relationships between the electrical characteristics of the circulator and the characteristics of ferrite have been clarified, thus, one is able to estimate the characteristics of the device from the ferrite. The further development of ferrite material to improve the low field loss and also linewidth in the future, will contribute to making a circulator with smaller insertion loss and more wide-band performance.

#### APPENDIX I

##### EIGENVALUES OF IMPEDANCE AND ADMITTANCE MATRIX OF ROTATIONALLY SYMMETRICAL CIRCUIT

Maxwell's equations in source free, are

$$\nabla \times H = j\omega \epsilon E \quad (36)$$

$$\nabla \times E = -j\omega \mathbf{u}H \quad (37)$$

Scalarly multiplying (37) by  $H^*$  and the conjugate of (36) by  $E$ , we obtain for the difference of the two resultant equations

$$\nabla \cdot H^* \times E = j\omega(H^* \mathbf{u}H - E \epsilon^* E^*). \quad (38)$$

Integrating (38) on the closed surface with  $n$  ports  $S_p$  ( $p=1, 2, 3, \dots, n$ )

$$\begin{aligned} \sum_{p=1}^n \iint_{S_p} H_{tp}^* \times E_{tp} \cdot n dS \\ = j\omega \iiint_{\tau} (H^* \mathbf{u}H - E \epsilon^* E^*) d\tau. \end{aligned} \quad (39)$$

In (39) subscript  $p$  denotes  $p$ th port and  $t$  denotes transverse field at each port. The fields on surface  $S_p$  are expressed with mode voltages  $v_p$ , mode currents  $i_p$  and normalized transverse mode vector  $e_t$ ,  $h_t$ . These relations are shown in the following.

$$E_{tp} = v_p e_t, \quad H_{tp} = i_p h_t \quad (40)$$

$$\begin{aligned} \iint_{S_p} |e_t|^2 dS &= \iint_{S_p} |h_t|^2 dS \\ &= - \iint_{S_p} n \cdot e_t \times h_t^* dS = 1 \end{aligned} \quad (41)$$

From 40 and 39,

$$\begin{aligned} \sum_{p=1}^n i_p^* v_p \iint_{S_p} (e_t \times h_t^*) \cdot (-n) \cdot dS \\ = j\omega \iiint_{\tau} (H^* \mathbf{u}H - E \epsilon^* E^*) d\tau. \end{aligned} \quad (42)$$

When the ports are excited by eigenvector, we have this relation at each port,

$$v_p = z j_p. \quad (43)$$

Since the eigenvector has the same amplitude at each port for the rotationally symmetry, for  $|i_p|=1$ , from (42) and (43), we get

$$z = \frac{j\omega}{n} \iiint_{\tau} (H^* \mathbf{u}H - E \epsilon^* E^*) d\tau. \quad (44)$$

When each port is excited by TEM mode, the  $i$ th eigenvalue of impedance matrix  $Z_i$  can be obtained from (44) as in

$$Z_i = \frac{j\omega}{n} \iiint_{\tau} (H_i^* \mathbf{u}H_i - E_i \epsilon^* E_i^*) d\tau. \quad (45)$$

In (45),  $H_i$  and  $E_i$  are the fields corresponding to the  $i$ th eigenvector with unit current. Similarly we get the eigenvalue of admittance matrix, as in

$$Y_i = \frac{j\omega}{n} \iiint_{\tau} (E_i \epsilon^* E_i^* - H_i^* \mathbf{u}H_i) d\tau \quad (46)$$

where  $E_i$  and  $H_i$  are the field corresponding to the eigenvector with unit voltage.

## APPENDIX II

FREQUENCY VARIATION OF EIGENVALUES OF  
PURE REACTANCE NETWORK

Taking the variation of (36) and (37), we get

$$\nabla \times \delta H - j\epsilon(\omega \cdot \delta E + E \cdot \delta \omega) - j\omega \cdot \delta \epsilon \cdot E = 0 \quad (47)$$

$$\nabla \times \delta E + j\mathbf{u}(\omega \cdot \delta H + H \cdot \delta \omega) + j\omega \cdot \delta \mathbf{u} H = 0. \quad (48)$$

Taking the difference between (47) and (48), and integrating on the closed surface with  $S_p$ , we get

$$\begin{aligned} & \sum_{p=1}^n \iint_{S_p} (E \times \delta H^* - \delta E \times H^*) \cdot (-n) dS \\ &= j\delta\omega \iint \int_{\tau} \left\{ E \left( \epsilon^* + \frac{\partial \epsilon^*}{\partial \omega} \omega \right) E^* \right. \\ & \quad \left. + H^* \left( \mathbf{u} + \frac{\partial \mathbf{u}}{\partial \omega} \omega \right) H \right\} d\tau \\ & \quad + j\omega \iint \int_{\tau} (H^* \mathbf{u} \delta H - \delta H^* \mathbf{u} H) d\tau \\ & \quad + j\omega \iint \int_{\tau} (E \epsilon^* \delta E^* - \delta E \epsilon^* E^*) d\tau. \quad (49) \end{aligned}$$

When the field is that of the eigenvector,  $v_p$  and  $i_p$  of (40) have the relation

$$y v_p = i_p. \quad (50)$$

Taking variation of (50), one gets

$$\delta y \cdot v_p + y \cdot \delta v_p = \delta i_p. \quad (51)$$

Substituting (40) and (51) into (49), one gets

$$\begin{aligned} & \delta y \sum_{p=1}^n |v_p|^2 + y \sum_{p=1}^n (v_p \delta v_p^* - v_p^* \delta v_p) \\ &= j\delta\omega \iint \int_{\tau} \left\{ E \left( \epsilon^* + \frac{\partial \epsilon^*}{\partial \omega} \omega \right) E^* \right. \\ & \quad \left. + \left( \mathbf{u} + \frac{\partial \mathbf{u}}{\partial \omega} \omega \right) H \right\} d\tau \\ & \quad + j\omega \iint \int_{\tau} (H^* \mathbf{u} \delta H - \delta H^* \mathbf{u} H) d\tau \\ & \quad + j\omega \iint \int_{\tau} (E \epsilon^* \delta E^* - \delta E \epsilon^* E^*) d\tau. \quad (52) \end{aligned}$$

The 1st term of the left and right hand side of (52) are both imaginary, and the 2nd and the 3rd term of the left and right hand side are real values. Therefore, when each port is excited by an eigenvector with unit voltage, from (52) one gets

$$\begin{aligned} \delta y = j \frac{\delta\omega}{n} \iint \int_{\tau} \left\{ E \left( \epsilon^* + \frac{\partial \epsilon^*}{\partial \omega} \omega \right) E^* \right. \\ \left. + H^* \left( \mathbf{u} + \frac{\partial \mathbf{u}}{\partial \omega} \omega \right) H \right\} d\tau. \quad (53) \end{aligned}$$

In the same procedure, the variation of eigenvalues of impedance matrix can be expressed by

$$\begin{aligned} \delta z = j \frac{\delta\omega}{n} \iint \int_{\tau} \left\{ E \left( \epsilon^* + \frac{\partial \epsilon^*}{\partial \omega} \omega \right) E^* \right. \\ \left. + H^* \left( \mathbf{u} + \frac{\partial \mathbf{u}}{\partial \omega} \omega \right) H \right\} d\tau. \quad (54) \end{aligned}$$

In the case

$$\frac{\partial \mathbf{u}}{\partial \omega} \omega \ll \mu, \quad \frac{\partial \epsilon^*}{\partial \omega} \omega \ll \epsilon^*,$$

we get

$$\delta y = j \frac{\delta\omega}{n} \iint \int_{\tau} (E \epsilon^* E^* + H^* \mathbf{u} H) d\tau \quad (55)$$

$$\delta z = j \frac{\delta\omega}{n} \iint \int_{\tau} (E \epsilon^* E^* + H^* \mathbf{u} H) d\tau. \quad (56)$$

The  $E$ ,  $H$  in (53) and (55) are the fields corresponding to unit current excitation, while those in (54) and (56) show the field for unit voltage excitation. The approximation of  $(\partial \mathbf{u} / \partial \omega) \omega \ll \mu$  is assured in the case of the operation under the strong dc magnetic field, and the approximation is easily verified from (15) assuming  $\sigma^2 \gg 1$ . In the case of ferrite,  $\omega(\partial \epsilon^* / \partial \omega)$  can be also neglected from  $\epsilon^*$ .

## APPENDIX III

MEASUREMENT OF  $\mu_{\pm}$ 

Three ports of the mesh part containing ferrite disks are excited by the eigenvector of (1), where a port of them is connected through a slotted line with standing-wave detector by which the impedance  $Z_i' = j\omega \mu_i \xi$  is measured. The measured values  $\mu_i$  are indicated with  $\times$  signs in Fig. 3. Since under a dc magnetic field sufficiently strong so that  $\mu_i \doteq 1$ , the mesh part becomes reciprocal,  $\xi$  can be also determined by the following technique. The variable reactance or adjustable line is connected to port 2, and it is adjusted so that the signal applied to port 1 does not appear to port 3. The terminal impedance at port 1 in this state is the eigenvalue  $j\omega \xi$ . This is easily understood by the fact that the eigenvalues of  $\mathbf{u}_2$  and  $\mathbf{u}_3$  take the same value for a reciprocal symmetry circuit and the linear combination of  $\mathbf{u}_2$  and  $\mathbf{u}_3$  can satisfy the previously mentioned state.

## APPENDIX IV

RELATION BETWEEN BANDWIDTH AND TOTAL REACTIVE  
ENERGY IN LUMPED ELEMENT CIRCULATOR

From (46) eigenvalues  $y_2$  and  $y_3$  are expressed by

$$\begin{aligned} y_2 &= \frac{2}{3} j\omega (\bar{W}_e - \bar{W}_{m_2}) = -j \frac{1}{\sqrt{3}}, \\ y_3 &= \frac{2}{3} j\omega (\bar{W}_e - \bar{W}_{m_3}) = j \frac{1}{\sqrt{3}}, \quad (57) \end{aligned}$$

where  $\bar{W}_e$  is a time average of electric energy contained in  $C$  and  $\bar{W}_{m_2}$ ,  $\bar{W}_{m_3}$  are magnetic energies in ferrite. Taking the expression of

$$\frac{\bar{W}_{m_2} + \bar{W}_{m_3}}{2} = \bar{W}_m, \quad \bar{W}_{t_2} = \bar{W}_e + \bar{W}_{m_2},$$

$$\bar{W}_{t_3} = \bar{W}_e + \bar{W}_{m_3}, \quad (58)$$

the time average of total reactive energies are expressed by

$$\bar{W}_{t_2} = 2\bar{W}_m + \frac{\sqrt{3}}{2\omega}, \quad \bar{W}_{t_3} = 2\bar{W}_m - \frac{\sqrt{3}}{2\omega}. \quad (59)$$

From (6) and (55), we get

$$|\delta s_2| = \frac{3}{2} |\delta y_2| = \bar{W}_{t_2} |\delta\omega|,$$

$$|\delta s_3| = \frac{3}{2} |\delta y_3| = \bar{W}_{t_3} |\delta\omega|. \quad (60)$$

However, since we have the relation  $|\delta s_1| = 0$  as shown in (20), substituting the relation and (60) and (59) into (5), one gets

$$|S''| = \frac{\delta\omega}{3} \cdot \bar{W}_t \sqrt{1 + \left(\frac{3}{2\omega\bar{W}_t}\right)^2},$$

$$\bar{W}_t = \frac{\bar{W}_{t_2} + \bar{W}_{t_3}}{2} = 2\bar{W}_m. \quad (61)$$

From (57), we can also get the relation

$$\bar{W}_{m_2} + \bar{W}_{m_3} = \bar{W}_t = 2\bar{W}_e = 3C. \quad (62)$$

Substituting (62) into (61), one gets

$$w = \frac{2\delta\omega}{\omega} = \frac{6|S''|}{\omega\bar{W}_t \sqrt{1 + \left(\frac{3}{2\omega\bar{W}_t}\right)^2}}$$

$$= \frac{2|S''|}{\omega C \sqrt{1 + \left(\frac{1}{2\omega C}\right)^2}}. \quad (63)$$

Since we can get the relation  $\omega C = 1/\sqrt{3}\eta$  from (7), applying it to (63), we get (8).

APPENDIX V

DETERMINATION OF CHARACTERISTICS OF CIRCULATOR BY MEASUREMENT OF  $\mu'_{eff}$  AND  $Q_{eff}$

The means of measurement and the technique of the determination are as follows.

1) Measurements of  $\mu'_{eff}$  and  $Q_{eff}$

As  $\mu'_{eff}$  is an equivalent permeability when dc magnetic field is applied along the wave propagation of a coaxial line filled with ferrite,  $\mu'_{eff}$  is obtainable by measuring the admittances of coaxial line with and without ferrite

at shortened end. The measurement is made for dc fields of several strengths.

The value of  $Q_{eff}$  is obtained by measuring the  $Q$  of resonator in both cases with and without ferrite by the following technique.

When signal is applied at  $SS'$  in Fig. 11(a), the amount of the signal at  $LL'$  takes the minimum value  $m$  as shown in Fig. 11(b) for the resonant state of the branched line with short end. The unloaded  $Q$  of the resonator with ferrite  $Q_0$  is obtained by the relation of

$$Q_0 = \frac{Q_L}{m}, \quad Q_L = \frac{f}{\Delta f}, \quad \text{using Fig. 11(b).}$$

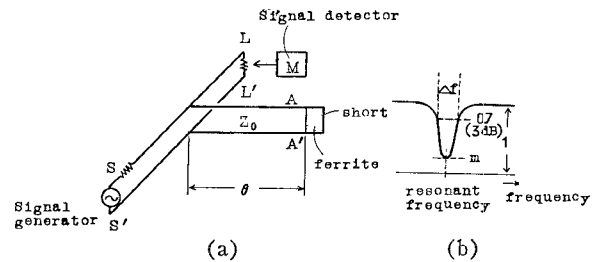


Fig. 11. Measurement of  $\mu'_{eff}$  and  $Q_{eff}$ .

The unloaded  $Q$  of the resonator without ferrite,  $Q_{cav}$ , is also obtained by the same way. So, one can get the value of  $Q_{eff}$  by

$$\frac{1}{Q_{eff}} = \left(\frac{1}{Q_0} - \frac{1}{Q_{cav}}\right) \frac{1}{k_f}$$

$$k_f = \frac{\bar{W}_f}{\bar{W}_t} = \text{filling factor}, \quad (64)$$

where  $\bar{W}_f$  is a magnetic energy in the part of ferrite, and  $\bar{W}_t$  is a total reactive energy inside the resonator.

However,  $k_f$  is obtainable by

$$k_f = \frac{\bar{W}_f}{\bar{W}_t} = \frac{X_f}{Z_0 \frac{\theta}{\cos^2 \theta} + X_f}$$

$$\theta = n\pi - \tan^{-1} \frac{X_f}{Z_0}, \quad (65)$$

where  $\frac{1}{X_f}$  is a imaginary part of the admittance at  $AA'$

with ferrite,  $n$  is the number of standing waves in resonator, and  $Z_0$  is a surge impedance of the coaxial line in the resonator.

2)  $\sigma$  is obtained from

$$\sigma = \frac{P}{\mu'_{eff} - 1}. \quad (66)$$

3) Insertion loss  $L(\text{dB})$  is obtained from

$$L(\text{dB}) = 4.98 \frac{\sigma(\sigma + P)}{P} \cdot \frac{1}{Q_{\text{eff}}} \quad (67)$$

4) Bandwidth ratio  $w$  is obtained from

$$w = 2\sqrt{3} |S''| \frac{P}{\sigma(\sigma + P)} \quad (68)$$

5) We get Fig. 10(a) from (61) and (68).

#### APPENDIX VI

REDUCTION OF  $y_3 - y_2$  BY POLDER'S EQUATION

$$\mu_{\pm} = 1 + \frac{4\pi M_s |\gamma|}{\omega(\sigma \mp 1)}, \quad \sigma = \frac{|\gamma| H_0}{\omega} \quad (69)$$

From (69)

$$\frac{1}{\mu_-} - \frac{1}{\mu_+} = \frac{4\pi M_s |\gamma|}{\omega} \cdot \frac{2}{\sigma^2 - 1} \cdot \frac{1}{1 + \frac{4\pi M_s |\gamma|}{\omega} \cdot \frac{2\sigma}{\sigma^2 - 1} + \frac{(4\pi M_s |\gamma|)^2}{\omega^2} \cdot \frac{1}{\sigma^2 - 1}} \quad (70)$$

Under the condition of  $4\pi M_s |\gamma|^2 / \omega \gg 1$  or  $\sigma^2 \gg 1$ ,

$$\frac{1}{\mu_-} - \frac{1}{\mu_+} = \frac{4\pi M_s \omega}{|\gamma| H_0^2} \cdot \frac{2}{\left(1 + \frac{4\pi M_s}{H_0}\right)^2} \quad (71)$$

However, we have the relation

$$\begin{aligned} y_3 - y_2 &= 2j\omega(\tilde{W}_{m_2}' - \tilde{W}_{m_3}') \\ &= 2j\omega \frac{1}{2\omega^2 \xi} \left( \frac{1}{\mu_-} - \frac{1}{\mu_+} \right) = j \frac{1}{\omega \xi} \left( \frac{1}{\mu_-} - \frac{1}{\mu_+} \right). \end{aligned} \quad (72)$$

Substituting (71) into (72),

$$y_3 - y_2 = j \frac{2}{\xi 4\pi M_s |\gamma| \left(1 + \frac{H_0}{4\pi M_s}\right)^2} \quad (73)$$

The value of  $y_3 - y_2$  is independent of the frequency.

#### ACKNOWLEDGMENT

The author wishes to express his appreciation to the Director of the Laboratories, Mr. Tatsuji Nomura, for his encouragement and advice in connection with this study. Thanks are also due to technical assistants of this Laboratory for taking the experimental data.

#### REFERENCES

- [1] U. Milano, J. H. Saunders, and L. Davis, Jr., "A Y-junction strip-line circulator," *IRE Trans. on Microwave Theory and Techniques*, vol. MTT-8, pp. 346-351, May 1960.
- [2] C. V. Beuhler and A. F. Eikenberg, "A VHF high-power Y-circulator," *IRE Trans. on Microwave Theory and Techniques (Correspondence)*, vol. MTT-9, pp. 569-570, November 1961.
- [3] Y. Konishi, I. Mochizuki, "Theory and design of Y-junction strip-line circulator," vol 15, no. 5, *Tech. J. Japan Broadcasting Corporation*, pp. 1-12, May 1963.
- [4] Y. Konishi, "Lumped element Y-circulator," *I.C.M.C.I. (Tokyo)*, pt. 1, M4-9, p. 61, September 1964.
- [5] Montgomery, Dicke, and Purcell, *Principles of Microwave Circuits*, New York: McGraw-Hill, 1948, p. 413.
- [6] B. A. Auld, "The synthesis of symmetrical waveguide circulators," *IRE Trans. on Microwave Theory and Techniques*, vol. MTT-7, pp. 238-246, April 1959.
- [7] H. Takahashi, "On the Ladder-Type Filter Network with Tchebycheff Response," *J. Institute of Electrical Communication Engineering of Japan*, pp. 65-76, February 1951.
- [8] Y. Konishi, "Wide band lumped element Y-circulator," *Institute of Electrical Communication Engineering of Japan Con. Rec.*, 4-1, 1964.